Editors' Suggestion

Overcoming Temperature Limits in the Optical Cooling of Solids Using Light-Dressed States

Luísa Toledo Tude, Conor N. Murphy, and Paul R. Eastham
School of Physics, Trinity College Dublin, Dublin 2, Ireland and
Trinity Quantum Alliance, Unit 16, Trinity Technology and Enterprise Centre, Pearse Street, Dublin 2, Ireland

(Received 29 September 2022; revised 25 July 2023; accepted 30 May 2024; published 27 June 2024)

Laser cooling of solids currently has a temperature floor of 50–100 K. We propose a method that could overcome this using defects, such as diamond color centers, with narrow electronic manifolds and bright optical transitions. It exploits the dressed states formed in strong fields which extend the set of phonon transitions and have tunable energies. This allows an enhancement of the cooling power and diminishes the effect of inhomogeneous broadening. We demonstrate these effects theoretically for the silicon vacancy and the germanium vacancy, and discuss the role of background absorption, phonon-assisted emission, and nonradiative decay.

DOI: 10.1103/PhysRevLett.132.266901

The optical cooling of solids to low temperatures is an important open challenge. The current method [1–3] is anti-Stokes fluorescence in rare-earth doped glasses [4]. In this process a rare-earth ion absorbs light, creating an excited electronic state which then absorbs phonons before reemitting the light at a higher frequency. Despite the competing heating by nonradiative decay and background absorption, temperatures as low as 91 K have been reached [3]. This is, however, reaching the fundamental limit of 50–100 K [4] set by the phonon energy that can be absorbed effectively. The same issue of a characteristic phonon energy also limits the possible cooling by absorption of optical phonons reported in room-temperature semiconductors [5,6] (see also Ref. [7]), and while various techniques have been considered to improve performance along with different cooling schemes [2,3,6,8–10], they do not address this problem. One route to reaching lower temperatures exploits the continuous electronic dispersion in semiconductors [11–15], but has yet to be achieved [7].

In this Letter, we propose a mechanism by which the temperature floor of solid-state laser cooling could be overcome, using quasiresonant excitation of a suitable defect state. We focus on the group IV color centers in diamond and in particular the negatively charged silicon-vacancy defect (SiV). The states of this defect comprise a ground-state and an excited-state manifold with dipole-active optical transitions between the two [16–19]. At sufficiently low temperatures the optical spectrum shows four lines, two of which could be resonantly driven to produce a form of anti-Stokes cooling. For weak driving this process is very sensitive to detuning. However, for stronger driving the dynamics becomes controlled by laser-dressed states rather than the original electronic eigenstates. The formation of these states, via the Autler-Townes effect [20], leads to a more complex cooling process with many phonon transitions occurring within the dressed-state spectrum [21]. This process, which we dub dressed state anti-Stokes cooling (DASC), corresponds to the inelastic scattering of the driving laser in the strong-driving regime. Importantly, it can be tuned to optimize the phonon absorption rates: by controlling the field intensity and detuning, the energy gaps and phonon matrix elements are modified in such a way that the coupling to the phonons is larger for the most occupied states at a given temperature. For the SiV we predict high gross cooling powers, of 1–100 fW per defect, down to temperatures of a few Kelvin. This is many orders-of-magnitude greater than could be achieved using rare-earth ions, even at the higher temperatures where they can operate. Furthermore, the cooling effect occurs over a broad range of detunings (see Fig. 1), and so survives in the presence of inhomogeneous broadening. While it will compete with various heating processes, as we discuss later, our results suggest DASC could enable the optical cooling of solids to temperatures unachievable with existing methods.

The SiV in diamond [18] is one of a family of group IV color centers [19] that are candidates for DASC. We focus on the SiV, although we obtain similar results for the germanium-vacancy (GeV) [21]. These defects are of interest for quantum nanophotonics, acting as both optically addressable spin qubits and effective single-photon emitters [25]. The electronic and spin states have long coherence times in the low temperature regime we consider, producing lifetime-limited spectra without spectral diffusion [18]. The spin coherence time for the SiV is submicrosecond due to phonon scattering within the ground-state manifold [18]. While this is disadvantageous for use as a spin qubit, it is beneficial for cooling because it allows rapid phonon absorption. Conventional anti-Stokes cooling using the SiV and related nitrogen vacancy (NV) was

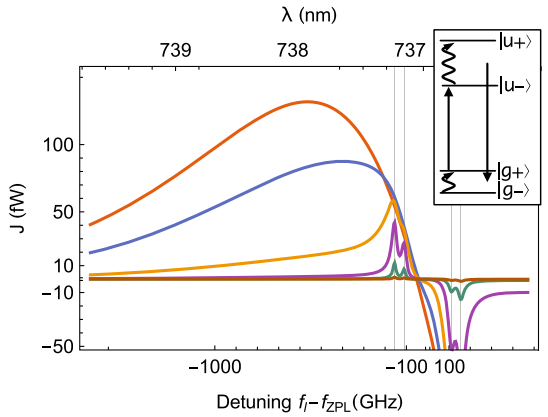

FIG. 1. Calculated cooling power of a single laser-driven SiV at $T = 20$ K, as a function of laser detuning. Different curves correspond to the different Rabi frequencies, i.e., driving strengths, $\Omega = 2 \times 10^{-0.5}, 2 \times 10^{-1}, \ldots, 2 \times 10^{-3}$ rad ps^{-1}. Rabi frequency decreases from the top to the bottom curves on the left of the plot. All polarizations are driven equally, $\Omega_z = \Omega_+ = \Omega_- = \Omega$. The vertical lines mark the four optical transitions between the ground-state and excited-state manifolds. The inset shows the spin-up levels of the SiV, and the anti-Stokes cooling process which occurs for weak driving on the lowest-energy transition. The cycle involves phonon transitions (wavy arrows), absorption of photons from the driving laser (straight upward arrow), and spontaneous emission (straight downward arrow).

considered in recent works [26,27], based on the broad absorption lines observed at room temperature. Here we consider, instead, high quality materials at low temperatures. This opens up the possibility of precision cooling approaches with tailored excitation of well-characterized transitions. Methods for cooling micromechanical resonators using the NV and SiV have been proposed [28,29], however, the goal in that case is to cool a single resonator mode, whereas we consider cooling of the bulk material.

A disadvantage of our method is that it will require precooling of the sample, unlike anti-Stokes cooling which operates from room temperature. Our analysis is restricted to a low temperature regime where we may use the Born-Markov approximation including only lowest-order single-phonon processes [21], and where heating due to nonradiative decay may not be overwhelming. For the SiV there is a strong decrease in the emission lifetime [30] above ~100 K, suggesting significant nonradiative decay which would preclude cooling. Another disadvantage of this type of defect is the presence of emission into phonon sidebands [18,25,31,32]. This will produce a competing heating effect, which would need to be suppressed using photonic structures [33–35].

To study optical cooling using an SiV we use an open-quantum systems description based on the Born-Markov approximation. As usual, we divide the problem into a system and baths, with the system Hamiltonian describing the SiV driven by a laser. It is a one-hole system with eight levels, four associated with spin-up and four with spin-down. The levels in each spin sector form an excited (u) and ground (g) state manifold, each containing two levels (see Fig. 1). The states in each manifold, $|u_\pm\rangle$ and $|g_\pm\rangle$, are split by the spin-orbit coupling constants $\lambda^u = 1.11$ and $\lambda^g = 0.19$ meV [16]. We ignore the small contribution of the linear vibronic Jahn-Teller interaction, which is around 5% of the spin-orbit coupling and so would not qualitatively affect our results. The manifolds are separated by the zero phonon line (ZPL) energy $E_{\rm ZPL} = 1.68$ eV, and coupled by electric-dipole optical transitions of various polarizations. We suppose that these transitions are driven by lasers of a single frequency ω_l, and use the Floquet representation obtained after a unitary transformation $U = e^{i\omega_l t(|u_+\rangle\langle u_+| + |u_-\rangle\langle u_-|)}$. The Hamiltonian for the spin-up sector is, with $\hbar = 1$,

$$H_S = \frac{1}{2}\begin{pmatrix} -\Delta + \lambda^u & 0 & \Omega_z & \Omega_+ \\ 0 & -\Delta - \lambda^u & \Omega_- & \Omega_z \\ \Omega_z & \Omega_- & \Delta + \lambda^g & 0 \\ \Omega_+ & \Omega_z & 0 & \Delta - \lambda^g \end{pmatrix}. \quad (1)$$

The basis here is in the order of decreasing energy in the original frame. In the Floquet basis the energies are shifted by the laser frequency, and given in terms of the detuning from the zero-phonon line $\Delta = \omega_l - \omega_{\rm ZPL}$. Ω_z is the Rabi frequency quantifying the strength of the driving with polarization along the z axis, which is the [111] crystal axis, and $\Omega_\pm$ are the Rabi frequencies for the two circular polarizations in the xy plane. The Hamiltonian for the spin-down sector is identical, except that the two circular polarizations are swapped. Most of our results refer to situations where $\Omega_+ = \Omega_-$, so that H_S describes both spin sectors.

Acoustic phonons cause transitions between states in each manifold due to the intramanifold coupling [29]

$$H_{I1} = \sum_k (f_k^u |u_+\rangle\langle u_-| + f_k^g |g_+\rangle\langle g_-| + \text{H.c.}) \otimes (a_k + a_k^\dagger). \quad (2)$$

They also affect the energy separation of the manifolds due to the intermanifold deformation-potential coupling [36,37]

$$H_{I2} = \sum_k g_k (|u_+\rangle\langle u_+| + |u_-\rangle\langle u_-| - |g_+\rangle\langle g_+| - |g_-\rangle\langle g_-|) \otimes (a_k + a_k^\dagger). \quad (3)$$

The bath has a super-Ohmic spectral density, reflecting the density of states of the acoustic phonons and the frequency dependence of the electron-phonon coupling. We use the expression [36,37] $J_p(\omega) = 2A\omega_c^{-2}\omega^3 e^{-\omega/\omega_c}$ with $A = 0.0275$ and $\omega_c = 2\pi$ rad ps^{-1}. We include only the bulk phonon contribution relevant to our results, neglecting the

local phonons which have much higher energies. The intermanifold coupling has been modeled [29] using the same form of $J_p(\omega)$ but with $A = 0.073$, reflecting the difference in matrix elements. We include this difference in the ratio f_k^u/g_k and for simplicity take $f_k^u = f_k^g$.

An equation of motion for the reduced density matrix of the SiV can be obtained using the Born-Markov approximation [38], which is well justified in the parameter regimes we consider [21]. The general form we use here is given in [21,39], along with the form for the mean heat current, from the phonons to the SiV, obtained using the method of full counting statistics [40]. The contribution to the heat current from phonon absorption is $J_{ab} = \sum_{ij} J_{ij}$,

$$J_{ij} \propto \nu_{ji} n(\nu_{ji}) J_p(\nu_{ji}), \tag{4}$$

where $\nu_{ji} = E_j - E_i$ are transition energies between the eigenstates of H_S, $J_p(\omega)$ is the phonon spectral density, and $n(\omega) = (e^{\beta\omega} - 1)^{-1}$ the occupation. We include the radiative decays using standard Lindblad dissipators [38], one for each transition from one of the u states to one of the g states. We neglect differences in the rates of the different decays, which are factors of order 1, and take them all to have rate $\gamma_0 = 1\ \mathrm{ns}^{-1}$ [41,42]. We drop the Lamb shift terms, which are negligible, but do not make the secular approximation.

Figure 1 shows the calculated cooling power as a function of driving frequency, for a single SiV at a temperature of 20 K, driven with $\Omega_z = \Omega_+ = \Omega_-$. Different curves correspond to different driving strengths, i.e., Rabi splittings, similar to those reached in experiments [43]. At weak driving, we see two characteristic peaks on each side of zero detuning, with those on the red (blue) side corresponding to net cooling (heating) of the phonons. The cooling (heating) effect corresponds to weak resonant driving of the two lowest (highest) of the four lines in the optical spectrum. As the driving is increased the red-detuned features first evolve into a broad spectral region where there is a very high cooling power. Further increases, beyond the driving strengths shown, then lead to a reduction in the maximum power.

Figure 2 shows the calculated maximum cooling power, obtained by maximizing over the detuning, as a function of temperature. We also show the corresponding values of the detuning. For weak driving, the optimal detuning is indistinguishable from that of the lowest-energy transition $|g_+\rangle \to |u_-\rangle$, $-(\lambda^u + \lambda^g)/2$, and is independent of temperature. This is consistent with the anti-Stokes cooling process illustrated in the inset to Fig. 1. For the lowest temperatures shown this process involves phonon transitions only in the ground-state manifold, giving a small cooling power. The cooling power increases as temperature is increased, allowing phonon absorption in the upper manifold, but then becomes constant, due to the presence of a characteristic maximum energy, λ^u, that can be

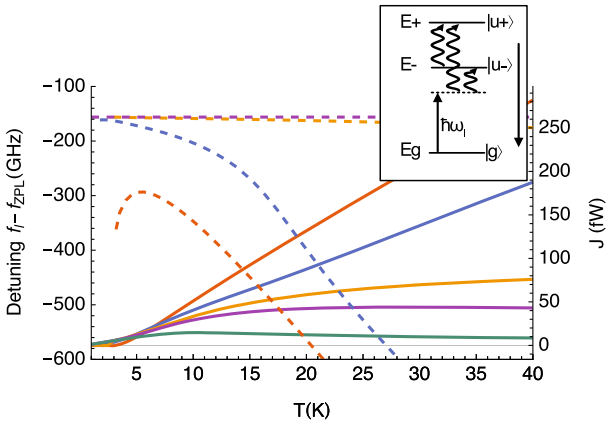

FIG. 2. Maximum cooling power (solid curves, right axis) and corresponding detuning (dashed curves, left axis) as a function of temperature for several driving strengths. Results are shown for $\Omega_z = \Omega_+ = \Omega_- = 2 \times 10^{-0.5}, 2 \times 10^{-1}, \ldots, 2 \times 10^{-2.5}$ rad ps^{-1}. The smallest Rabi frequency corresponds to the smallest power on the right of the plot, and the largest (least negative) detuning. The detuning curves for the two smallest Rabi frequencies coincide. The inset illustrates the quasienergies for a three-level model and the DASC cycle.

absorbed per cycle at weak driving. This saturation is absent in the strong-driving case, where the cooling power increases linearly with temperature. The optimal detuning is lower (more negative) than in the weak-driving case, corresponding to driving on the red side of the lowest-energy transition, and is strongly temperature dependent, becoming more negative as temperature increases.

The enhancement of the cooling power arises because for strong driving the heat flow to the phonons is controlled by transitions between the laser-dressed states, whose quasienergies are the eigenvalues of H_S. As can be seen in Eq. (4), each pair of states i, j gives rise to a heat flow proportional to the transition frequency, ν_{ji}, and the Bose function and spectral density at that frequency. Thus, by tuning the quasienergies through the driving field, we can increase the heat absorption beyond the maximum achievable with a fixed level structure.

In the four-level system there are multiple phonon absorption pathways, leading to a complex cooling cycle discussed further in the Supplemental Material [21]. However, we obtain similar results for a simplified three-level model with a single ground state and two excited states. This allows us to identify the essential features of the DASC process as those illustrated in the inset of Fig. 2. The eigenstates of the defect, in the presence of the periodic driving, are the Floquet states, with quasienergies defined up to integer multiples of the driving frequency. This introduces a periodic replica of the ground state, near to the excited states. The driving field then mixes the states together. Referring to Fig. 2 we see that, over the temperature regime shown, the driving strength is a fraction of the detuning, so the mixing produces only small energy

shifts. However, it gives rise to the two additional cooling processes, in which a photon and phonon are simultaneously absorbed. In terms of the original (undressed) states, these are Raman transitions from the ground to the excited states via a virtual intermediate state. The energy of the absorbed phonon in the two cases is approximately $(E_{\mp} - E_g) - \hbar\omega_l$, and can be tuned to maximize the cooling power. The increase in cooling power in Fig. 2 over the weak-driving case in the regime $kT \gtrsim \lambda^u$ arises because the larger transition energies increase the heat absorption. The transition energies can also be smaller than those in the bare spectrum, allowing cooling at temperatures below the limit set by the bare level splitting. Indeed, as can be inferred from the illustration, DASC can occur in a two-level system.

There is a maximum in the cooling power as a function of driving strength because the relaxation processes, and therefore the heat flows, depend on the dressed-state energies and compositions [44]. At large Ω the phonon heat current changes sign, and the cycle operates as a heater. For a two-level model one can define an effective temperature for the photons, whose relation to temperature of the phonon bath determines the direction of heat flow [45].

The cooling will compete with heating due to background absorption in the host material. The Rabi frequency $\hbar\Omega = dE_0$, where d is the transition dipole moment and E_0 the electric field amplitude, and the intensity is $I = c\epsilon_0 n E_0^2/2$. The heating rate due to background absorption, per SiV, is then $c\epsilon_0 n\hbar^2\Omega^2\alpha_b/(2d^2\rho)$, where α_b is the background absorption coefficient and ρ the SiV density. Considering the strongest field used in Fig. 1, we have a heating power $\sim 10^{25}(\alpha_b/\rho)$ fW m^{-2}, against a cooling power of $\sim$100 fW. Taking a conservative background absorption coefficient $\alpha_b = 0.1$ cm^{-1} [46], and $d = 14.3$ D [18] we then predict net cooling for $\rho \gtrsim 10^{24}$ m^{-3}, or about one SiV per 10^5 carbon atoms. Thus background heating is unlikely to be a limitation.

A second competing heating effect arises from radiative decay accompanied by the emission of phonons. In general, only a fraction α of the radiative decay is into the ZPL, with the remainder into the phonon sideband. For DASC, the maximum cooling power is limited by the radiative decay rate into the ZPL, and so is $\sim kT\alpha\gamma_0 p_u$, where p_u is the probability of occupying the upper manifold. The heating rate by sideband emission, with mean phonon energy $\bar{E}_{sb}$, is $\sim(1-\alpha)\gamma_0 p_u \bar{E}_{sb}$, so net cooling requires $\alpha > \bar{E}_{sb}/(\bar{E}_{sb} + kT)$. For the SiV, there is a strong effect of a local phonon with energy $\approx$60 meV [37], so at 30 K net cooling occurs if $\alpha > 0.95$. Many works [19,30,31,47,48] suggest $\alpha \approx 0.7$, however, $\alpha \approx 0.9$ has been reported [18,25]. Furthermore, α can be increased by using photonic structures [33–35].

A third competing heating effect is nonradiative decay from the u to the g manifold. The impact of this will be similar to that in conventional laser cooling [4]. A nonradiative decay with rate γ_{NR} implies heating $E_{\mathrm{ZPL}}\gamma_{\mathrm{NR}} p_u$. Net cooling at 10 K then requires $(\gamma_0 + \gamma_{\mathrm{NR}})/\gamma_{\mathrm{NR}} > E_{\mathrm{ZPL}}/kT \gtrsim 1000$, or a quantum efficiency (QE) of at least 99.9%. Experimental results for the QE in the low-temperature regime relevant here are scarce, although a lower bound on the QE of 30% has been found [18] from the measured lifetime and dipole moment. However, significantly longer lifetimes have been measured [41], which would imply much higher QEs, as would the rates from fits to second-order coherence data [17]. A value of 67% was found in room-temperature experiments [34], again implying a high QE at low temperatures, where the activated nonradiative processes disappear. Given these results we suggest that the QE required for cooling is achievable, with the low values in the literature perhaps due to extrinsic effects such as strain. We note also recent measurements of the Germanium vacancy [49–51] which suggest a high QE. We have investigated cooling in this defect and obtain results similar to those for the SiV [21].

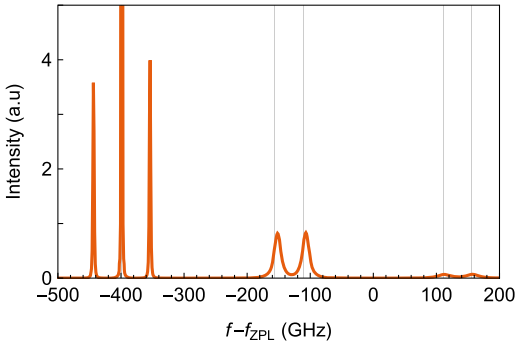

FIG. 3. Computed spectrum of the light from an SiV at 20 K driven with $\Omega_+ = \Omega_- = \Omega_z = 2\times10^{-1}$ rad ps^{-1}. This corresponds to the second-highest driving shown in Fig. 1. The laser is detuned to the maximum in the cooling power at $f_l - f_{\mathrm{ZPL}} = -400$ GHz. All polarization components have been combined to show the total power.

The DASC process could be observed via the scattering of the driving laser. Figure 3 shows the spectrum of the light from an SiV driven in the cooling regime. It contains two sidebands around the laser frequency, forming a Mollow triplet [52], and four broader peaks near to the original emission lines. The scattered intensity at frequencies above the driving, at $f_l = -400$ GHz, is greater than that below it, so on average the scattering increases the energy of the photons. The energy they gain corresponds, by energy conservation, to that lost by the phonons, and this blueshifting of the scattering demonstrates that heat is being removed from the crystal.

In conclusion, we have proposed and analyzed an approach to the optical cooling of solids using quasiresonant excitation of optically active defect states in a low-temperature regime. Our approach could overcome the temperature limitations inherent in optical cooling using

rare-earths, set by the gaps within the electronic manifolds, by using laser dressing to control the frequencies of the phonon transitions. This allows the process to take advantage of the maximum in the phonon heat absorption rate for transition energies $\sim kT$ and so produce a large cooling power. This could allow systems such as the group-IV color centers in diamond to cool effectively. The dressed-state enhancement, along with the fast radiative rates, leads to predicted cooling powers many orders of magnitude greater than could be obtained using rare-earths, down to temperatures of a few Kelvin. An interesting question is the maximum temperature at which these processes could be effective. While the Born-Markov theory will eventually break down, it is likely that the upper limit in practice will be set by the breakdown of the four-level model and the absorption and decay arising from other states [21].

We acknowledge funding from the Irish Research Council under Award GOIPG/2017/1091, and Science Foundation Ireland (21/FFP-P/10142).

L. T. T. and C. N. M. contributed equally to this work.

[1] R. I. Epstein, M. I. Buchwald, B. C. Edwards, T. R. Gosnell, and C. E. Mungan, Observation of laser-induced fluorescent cooling of a solid, Nature (London) **377**, 500 (1995).
[2] D. V. Seletskiy, S. D. Melgaard, S. Bigotta, A. Di Lieto, M. Tonelli, and M. Sheik-Bahae, Laser cooling of solids to cryogenic temperatures, Nat. Photonics **4**, 161 (2010).
[3] S. D. Melgaard, A. R. Albrecht, M. P. Hehlen, and M. Sheik-Bahae, Solid-state optical refrigeration to sub-100 Kelvin regime, Sci. Rep. **6**, 20380 (2016).
[4] D. V. Seletskiy, R. Epstein, and M. Sheik-Bahae, Laser cooling in solids: Advances and prospects, Rep. Prog. Phys. **79**, 096401 (2016).
[5] J. Zhang, D. Li, R. Chen, and Q. Xiong, Laser cooling of a semiconductor by 40 Kelvin, Nature (London) **493**, 504 (2013).
[6] J. Zhang, Q. Zhang, X. Wang, L. C. Kwek, and Q. Xiong, Resolved-sideband Raman cooling of an optical phonon in semiconductor materials, Nat. Photonics **10**, 600 (2016).
[7] Y. V. Morozov, S. Zhang, A. Pant, B. Jankó, S. D. Melgaard, D. A. Bender, P. J. Pauzauskie, and M. Kuno, Can lasers really refrigerate CdS nanobelts?, Nature (London) **570**, E60 (2019).
[8] N. Vermeulen, C. Debaes, P. Muys, and H. Thienpont, Mitigating heat dissipation in Raman lasers using coherent anti-Stokes Raman scattering, Phys. Rev. Lett. **99**, 093903 (2007).
[9] S. C. Rand, Raman laser cooling of solids, J. Lumin. **133**, 10 (2013).
[10] L. B. Andre, L. Cheng, and S. C. Rand, Saturation, allowed transitions and quantum interference in laser cooling of solids, Appl. Sci. **12**, 953 (2022).
[11] M. Sheik-Bahae and R. I. Epstein, Can laser light cool semiconductors?, Phys. Rev. Lett. **92**, 247403 (2004).
[12] L. A. Rivlin and A. A. Zadernovsky, Laser cooling of semiconductors, Opt. Commun. **139**, 219 (1997).
[13] E. Finkeißen, M. Potemski, P. Wyder, L. Viña, and G. Weimann, Cooling of a semiconductor by luminescence up-conversion, Appl. Phys. Lett. **75**, 1258 (1999).
[14] G. Rupper, N. H. Kwong, and R. Binder, Theory of semiconductor laser cooling at low temperatures, Phys. Status Solidi C **3**, 2489 (2006).
[15] G. Rupper, N. H. Kwong, and R. Binder, Large excitonic enhancement of optical refrigeration in semiconductors, Phys. Rev. Lett. **97**, 117401 (2006).
[16] C. Hepp, T. Müller, V. Waselowski, J. N. Becker, B. Pingault, H. Sternschulte, D. Steinmüller-Nethl, A. Gali, J. R. Maze, M. Atatüre, and C. Becher, Electronic structure of the silicon vacancy color center in diamond, Phys. Rev. Lett. **112**, 036405 (2014).
[17] E. Neu, C. Hepp, M. Hauschild, S. Gsell, M. Fischer, H. Sternschulte, D. Steinmüller-Nethl, M. Schreck, and C. Becher, Low-temperature investigations of single silicon vacancy colour centres in diamond, New J. Phys. **15**, 043005 (2013).
[18] J. N. Becker and C. Becher, Coherence properties and quantum control of silicon vacancy color centers in diamond, Phys. Status Solidi A **214**, 1700586 (2017).
[19] C. Bradac, W. Gao, J. Forneris, M. E. Trusheim, and I. Aharonovich, Quantum nanophotonics with group IV defects in diamond, Nat. Commun. **10**, 5625 (2019).
[20] S. H. Autler and C. H. Townes, Stark effect in rapidly varying fields, Phys. Rev. **100**, 703 (1955).
[21] See Supplemental Material at http://link.aps.org/supplemental/10.1103/PhysRevLett.132.266901, which includes Refs. [22–24], for details of the method and additional results.
[22] M. Popovic, M. T. Mitchison, A. Strathearn, B. W. Lovett, J. Goold, and P. R. Eastham, Quantum heat statistics with time-evolving matrix product operators, PRX Quantum **2**, 020338 (2021).
[23] E. M. Gauger and J. Wabnig, Heat pumping with optically driven excitons, Phys. Rev. B **82**, 073301 (2010).
[24] C. N. Murphy and P. R. Eastham, Quantum control of excitons for reversible heat transfer, Commun. Phys. **2**, 120 (2019).
[25] E. Neu, D. Steinmetz, J. Riedrich-Möller, S. Gsell, M. Fischer, M. Schreck, and C. Becher, Single photon emission from silicon-vacancy colour centres in chemical vapour deposition nano-diamonds on iridium, New J. Phys. **13**, 025012 (2011).
[26] M. Kern, J. Jeske, D. W. M. Lau, A. D. Greentree, F. Jelezko, and J. Twamley, Optical cryocooling of diamond, Phys. Rev. B **95**, 235306 (2017).
[27] Y.-F. Gao, Q.-H. Tan, X.-L. Liu, S.-L. Ren, Y.-J. Sun, D. Meng, Y.-J. Lu, P.-H. Tan, C.-X. Shan, and J. Zhang, Phonon-assisted photoluminescence up-conversion of silicon-vacancy centers in diamond, J. Phys. Chem. Lett. **9**, 6656 (2018).
[28] K. V. Kepesidis, S. D. Bennett, S. Portolan, M. D. Lukin, and P. Rabl, Phonon cooling and lasing with nitrogen-vacancy centers in diamond, Phys. Rev. B **88**, 064105 (2013).

[29] K. V. Kepesidis, M.-A. Lemonde, A. Norambuena, J. R. Maze, and P. Rabl, Cooling phonons with phonons: Acoustic reservoir engineering with silicon-vacancy centers in diamond, Phys. Rev. B **94**, 214115 (2016).
[30] K. D. Jahnke, A. Sipahigil, J. M. Binder, M. W. Doherty, M. Metsch, L. J. Rogers, N. B. Manson, M. D. Lukin, and F. Jelezko, Electron-phonon processes of the silicon-vacancy centre in diamond, New J. Phys. **17**, 043011 (2015).
[31] E. Londero, G. Thiering, L. Razinkovas, A. Gali, and A. Alkauskas, Vibrational modes of negatively charged silicon-vacancy centers in diamond from *ab initio* calculations, Phys. Rev. B **98**, 035306 (2018).
[32] J. Görlitz, D. Herrmann, G. Thiering, P. Fuchs, M. Gandil, T. Iwasaki, T. Taniguchi, M. Kieschnick, J. Meijer, M. Hatano, A. Gali, and C. Becher, Spectroscopic investigations of negatively charged tin-vacancy centres in diamond, New J. Phys. **22**, 013048 (2020).
[33] L. Ondič, M. Varga, J. Fait, K. Hruška, V. Jurka, A. Kromka, J. Maňák, P. Kapusta, and J. Nováková, Photonic crystal cavity-enhanced emission from silicon vacancy centers in polycrystalline diamond achieved without postfabrication fine-tuning, Nanoscale **12**, 13055 (2020).
[34] J. Riedrich-Möller, C. Arend, C. Pauly, F. Mücklich, M. Fischer, S. Gsell, M. Schreck, and C. Becher, Deterministic coupling of a single silicon-vacancy color center to a photonic crystal cavity in diamond, Nano Lett. **14**, 5281 (2014).
[35] M. Ruf, M. J. Weaver, S. B. van Dam, and R. Hanson, Resonant excitation and Purcell enhancement of coherent nitrogen-vacancy centers coupled to a Fabry-Perot microcavity, Phys. Rev. Appl. **15**, 024049 (2021).
[36] A. Norambuena, J. R. Maze, P. Rabl, and R. Coto, Quantifying phonon-induced non-Markovianity in color centers in diamond, Phys. Rev. A **101**, 022110 (2020).
[37] A. Norambuena, S. A. Reyes, J. Mejía-Lopéz, A. Gali, and J. R. Maze, Microscopic modeling of the effect of phonons on the optical properties of solid-state emitters, Phys. Rev. B **94**, 134305 (2016).
[38] H.-P. Breuer and F. Petruccione, *The Theory of Open Quantum Systems* (Oxford University Press, New York, 2007).
[39] C. N. Murphy, L. Toledo Tude, and P. R. Eastham, Laser cooling beyond rate equations: Approaches from quantum thermodynamics, Appl. Sci. **12**, 1620 (2022).
[40] M. Esposito, U. Harbola, and S. Mukamel, Nonequilibrium fluctuations, fluctuation theorems, and counting statistics in quantum systems, Rev. Mod. Phys. **81**, 1665 (2009).
[41] H. Sternschulte, K. Thonke, R. Sauer, P. C. Münzinger, and P. Michler, 1.681-eV luminescence center in chemical-vapor-deposited homoepitaxial diamond films, Phys. Rev. B **50**, 14554 (1994).
[42] C. Wang, C. Kurtsiefer, H. Weinfurter, and B. Burchard, Single photon emission from SiV centres in diamond produced by ion implantation, J. Phys. B **39**, 37 (2005).
[43] Y. Zhou, A. Rasmita, K. Li, Q. Xiong, I. Aharonovich, and W.-b. Gao, Coherent control of a strongly driven silicon vacancy optical transition in diamond, Nat. Commun. **8**, 14451 (2017).
[44] E. Geva and R. Kosloff, Three-level quantum amplifier as a heat engine: A study in finite-time thermodynamics, Phys. Rev. E **49**, 3903 (1994).
[45] C. Murphy, Quantum control of thermodynamic processes in semiconductors, Ph.D. thesis, Trinity College Dublin, 2022.
[46] M. E. Thomas, Multiphonon model for absorption in diamond, in *Window and Dome Technologies and Materials IV*, edited by P. Klocek, International Society for Optics and Photonics Vol. 2286 (SPIE, San Diego, CA, 1994), pp. 152–159.
[47] B. C. Rose, D. Huang, Z.-H. Zhang, P. Stevenson, A. M. Tyryshkin, S. Sangtawesin, S. Srinivasan, L. Loudin, M. L. Markham, A. M. Edmonds, D. J. Twitchen, S. A. Lyon, and N. P. de Leon, Observation of an environmentally insensitive solid-state spin defect in diamond, Science **361**, 60 (2018).
[48] S. Häußler, G. Thiering, A. Dietrich, N. Waasem, T. Teraji, J. Isoya, T. Iwasaki, M. Hatano, F. Jelezko, A. Gali, and A. Kubanek, Photoluminescence excitation spectroscopy of SiV- and GeV- color center in diamond, New J. Phys. **19**, 063036 (2017).
[49] M. K. Bhaskar, D. D. Sukachev, A. Sipahigil, R. E. Evans, M. J. Burek, C. T. Nguyen, L. J. Rogers, P. Siyushev, M. H. Metsch, H. Park, F. Jelezko, M. Loncar, and M. D. Lukin, Quantum nonlinear optics with a germanium-vacancy color center in a nanoscale diamond waveguide, Phys. Rev. Lett. **118**, 223603 (2017).
[50] Y. N. Palyanov, I. N. Kupriyanov, Y. M. Borzdov, and N. V. Surovtsev, Germanium: A new catalyst for diamond synthesis and a new optically active impurity in diamond, Sci. Rep. **5**, 14789 (2015).
[51] T. Iwasaki, F. Ishibashi, Y. Miyamoto, Y. Doi, S. Kobayashi, T. Miyazaki, K. Tahara, K. D. Jahnke, L. J. Rogers, B. Naydenov, F. Jelezko, S. Yamasaki, S. Nagamachi, T. Inubushi, N. Mizuochi, and M. Hatano, Germanium-vacancy single color centers in diamond, Sci. Rep. **5**, 12882 (2015).
[52] B. R. Mollow, Power spectrum of light scattered by two-level systems, Phys. Rev. **188**, 1969 (1969).